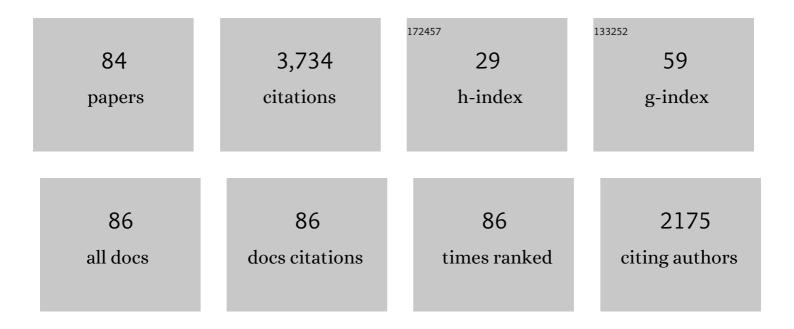
List of Publications by Year in descending order

Source: https://exaly.com/author-pdf/2574456/publications.pdf Version: 2024-02-01



#	Article	IF	CITATIONS
1	Hayabusa2 arrives at the carbonaceous asteroid 162173 Ryugu—A spinning top–shaped rubble pile. Science, 2019, 364, 268-272.	12.6	410
2	The geomorphology, color, and thermal properties of Ryugu: Implications for parent-body processes. Science, 2019, 364, 252.	12.6	313
3	Lunar Global Shape and Polar Topography Derived from Kaguya-LALT Laser Altimetry. Science, 2009, 323, 897-900.	12.6	263
4	Possible mantle origin of olivine around lunar impact basins detected by SELENE. Nature Geoscience, 2010, 3, 533-536.	12.9	184
5	Farside Gravity Field of the Moon from Four-Way Doppler Measurements of SELENE (Kaguya). Science, 2009, 323, 900-905.	12.6	169
6	Sample collection from asteroid (162173) Ryugu by Hayabusa2: Implications for surface evolution. Science, 2020, 368, 654-659.	12.6	158
7	Preliminary analysis of the Hayabusa2 samples returned from C-type asteroid Ryugu. Nature Astronomy, 2022, 6, 214-220.	10.1	136
8	Timing and characteristics of the latest mare eruption on the Moon. Earth and Planetary Science Letters, 2011, 302, 255-266.	4.4	133
9	Crustal thickness of the Moon: Implications for farside basin structures. Geophysical Research Letters, 2009, 36, .	4.0	102
10	Massive layer of pure anorthosite on the Moon. Geophysical Research Letters, 2012, 39, .	4.0	102
11	Highly porous nature of a primitive asteroid revealed by thermal imaging. Nature, 2020, 579, 518-522.	27.8	100
12	Samples returned from the asteroid Ryugu are similar to Ivuna-type carbonaceous meteorites. Science, 2023, 379, .	12.6	97
13	An improved lunar gravity field model from SELENE and historical tracking data: Revealing the farside gravity features. Journal of Geophysical Research, 2010, 115, .	3.3	92
14	Illumination conditions of the south pole of the Moon derived using Kaguya topography. Icarus, 2010, 208, 558-564.	2.5	88
15	Internal structure of the Moon inferred from Apollo seismic data and selenodetic data from GRAIL and LLR. Geophysical Research Letters, 2015, 42, 7351-7358.	4.0	88
16	Illumination conditions at the lunar polar regions by KAGUYA(SELENE) laser altimeter. Geophysical Research Letters, 2008, 35, .	4.0	86
17	Pebbles and sand on asteroid (162173) Ryugu: In situ observation and particles returned to Earth. Science, 2022, 375, 1011-1016.	12.6	78
18	On the origin and evolution of the asteroid Ryugu: A comprehensive geochemical perspective. Proceedings of the Japan Academy Series B: Physical and Biological Sciences, 2022, 98, 227-282.	3.8	77

#	Article	IF	CITATIONS
19	Lunar gravity field determination using SELENE same-beam differential VLBI tracking data. Journal of Geodesy, 2011, 85, 205-228.	3.6	63
20	Olivine-rich exposures in the South Pole-Aitken Basin. Icarus, 2012, 218, 331-344.	2.5	57
21	Mare volcanism in the lunar farside Moscoviense region: Implication for lateral variation in magma production of the Moon. Geophysical Research Letters, 2009, 36, .	4.0	51
22	Geologic structure generated by largeâ€impact basin formation observed at the South Poleâ€Aitken basin on the Moon. Geophysical Research Letters, 2014, 41, 2738-2745.	4.0	49
23	Thermally altered subsurface material of asteroid (162173) Ryugu. Nature Astronomy, 2021, 5, 246-250.	10.1	47
24	Compositional evidence for an impact origin of the Moon's Procellarum basin. Nature Geoscience, 2012, 5, 775-778.	12.9	45
25	Picosecond accuracy VLBI of the two subsatellites of SELENE (KAGUYA) using multifrequency and same beam methods. Radio Science, 2009, 44, .	1.6	38
26	A new type of pyroclastic deposit on the Moon containing Feâ€ s pinel and chromite. Geophysical Research Letters, 2013, 40, 4549-4554.	4.0	38
27	Development of an application scheme for the SELENE/SP lunar reflectance model for radiometric calibration of hyperspectral and multispectral sensors. Planetary and Space Science, 2016, 124, 76-83.	1.7	33
28	The 1998 Miyako fireball's trajectory determined from shock wave records of a dense seismic array. Earth, Planets and Space, 2003, 55, e9-e12.	2.5	32
29	The relative timing of Lunar Magma Ocean solidification and the Late Heavy Bombardment inferred from highly degraded impact basin structures. Icarus, 2015, 250, 492-503.	2.5	30
30	Anomalously porous boulders on (162173) Ryugu as primordial materials from its parent body. Nature Astronomy, 2021, 5, 766-774.	10.1	30
31	The 2003 Kanto large bolide's trajectory determined from shockwaves recorded by a seismic network and images taken by a video camera. Geophysical Research Letters, 2004, 31, .	4.0	26
32	Lunar farside Th distribution measured by Kaguya gamma-ray spectrometer. Earth and Planetary Science Letters, 2012, 337-338, 10-16.	4.4	23
33	Anomalous Moscoviense basin: Single oblique impact or double impact origin?. Geophysical Research Letters, 2011, 38, n/a-n/a.	4.0	22
34	Viscoelastic deformation of lunar impact basins: Implications for heterogeneity in the deep crustal paleoâ€ŧhermal state and radioactive element concentration. Journal of Geophysical Research E: Planets, 2013, 118, 398-415.	3.6	22
35	Evidence of impact melt sheet differentiation of the lunar South Poleâ€Aitken basin. Journal of Geophysical Research E: Planets, 2017, 122, 1672-1686.	3.6	22
36	Azimuthally controlled observation of heavy cosmic-ray primaries by means of the balloon-borne emulsion chamber. Astroparticle Physics, 1997, 6, 155-167.	4.3	21

#	Article	IF	CITATIONS
37	Capability of the penetrator seismometer system for lunar seismic event observation. Planetary and Space Science, 2009, 57, 751-763.	1.7	21
38	An Overview of JAXA's Ground-Observation Activities for HAYABUSA Reentry. Publication of the Astronomical Society of Japan, 2011, 63, 961-969.	2.5	21
39	Detection of Acoustic/Infrasonic/Seismic Waves Generated by Hypersonic Re-Entry of the HAYABUSA Capsule and Fragmented Parts of the Spacecraft. Publication of the Astronomical Society of Japan, 2011, 63, 971-978.	2.5	20
40	Same-beam VLBI observations of SELENE for improving lunar gravity field model. Radio Science, 2010, 45, n/a-n/a.	1.6	19
41	Hayabusa2 Landing Site Selection: Surface Topography of Ryugu and Touchdown Safety. Space Science Reviews, 2020, 216, 1.	8.1	17
42	Infrasound/seismic observation of the Hayabusa reentry: Observations and preliminary results. Earth, Planets and Space, 2012, 64, 655-660.	2.5	16
43	Infrasound observations at Syowa Station, East Antarctica: Implications for detecting the surface environmental variations in the polar regions. Geoscience Frontiers, 2015, 6, 285-296.	8.4	16
44	Improving Hayabusa2 trajectory by combining LIDAR data and a shape model. Icarus, 2020, 338, 113574.	2.5	16
45	Analytical and graphical determination of the trajectory of a fireball using seismic data. Planetary and Space Science, 2006, 54, 78-86.	1.7	15
46	Seismic Wave Interactions Between the Atmosphere - Ocean - Cryosphere System and the Geosphere in Polar Regions. , 0, , .		14
47	Global occurrence trend of high-Ca pyroxene on lunar highlands and its implications. Journal of Geophysical Research E: Planets, 2015, 120, 831-848.	3.6	13
48	Featureless spectra on the Moon as evidence of residual lunar primordial crust. Journal of Geophysical Research E: Planets, 2015, 120, 2190-2205.	3.6	13
49	Infrasound array observations in the Lützow-Holm Bay region, East Antarctica. Polar Science, 2015, 9, 35-50.	1.2	13
50	Albedo Observation by Hayabusa2 LIDAR: Instrument Performance and Error Evaluation. Space Science Reviews, 2017, 208, 49-64.	8.1	13
51	Lunar laser topography by LALT on board the KAGUYA lunar explorer – Operational history, new topographic data, peak height analysis of laser echo pulses. Advances in Space Research, 2013, 52, 262-271.	2.6	12
52	Variation of the lunar highland surface roughness at baseline 0.15–100 km and the relationship to relative age. Geophysical Research Letters, 2014, 41, 1444-1451.	4.0	11
53	Dust Detection Mode of the Hayabusa2 LIDAR. Space Science Reviews, 2017, 208, 65-79.	8.1	11
54	Dynamic precise orbit determination of Hayabusa2 using laser altimeter (LIDAR) and image tracking data sets. Earth, Planets and Space, 2020, 72, .	2.5	11

#	Article	IF	CITATIONS
55	Overview of Differential VLBI Observations of Lunar Orbiters in SELENE (Kaguya) for Precise Orbit Determination and Lunar Gravity Field Study. Space Science Reviews, 2010, 154, 123-144.	8.1	9
56	Accuracy assessment of lunar topography models. Earth, Planets and Space, 2011, 63, 15-23.	2.5	9
57	Numerical Simulation of Lunar Seismic Wave Propagation: Investigation of Subsurface Scattering Properties Near Apollo 12 Landing Site. Journal of Geophysical Research E: Planets, 2021, 126, e2020JE006406.	3.6	9
58	Time–space variations in infrasound sources related to environmental dynamics around Lützow–Holm Bay, east Antarctica. Polar Science, 2017, 14, 39-48.	1.2	8
59	Global classification of lunar reflectance spectra obtained by Kaguya (SELENE): Implication for hidden basaltic materials. Icarus, 2019, 321, 407-425.	2.5	8
60	Improving the geometry of Kaguya extended mission data through refined orbit determination using laser altimetry. Icarus, 2020, 336, 113454.	2.5	8
61	Infrasonic Waves in Antarctica: A New Proxy for Monitoring Polar Environment. International Journal of Geosciences, 2013, 04, 797-802.	0.6	8
62	Light detection and ranging (LIDAR) laser altimeter for the Martian Moons Exploration (MMX) spacecraft. Earth, Planets and Space, 2021, 73, .	2.5	7
63	Constraints on timing and magnitude of early global expansion of the Moon from topographic features in linear gravity anomaly areas. Geophysical Research Letters, 2016, 43, 4865-4870.	4.0	6
64	Infrasound Signals and Their Source Location Inferred from Array Deployment in the Lützow-Holm Bay Region, East Antarctica: January-June 2015. International Journal of Geosciences, 2017, 08, 181-188.	0.6	6
65	The scientific observation campaign of the Hayabusa-2 capsule re-entry. Publication of the Astronomical Society of Japan, 2022, 74, 50-63.	2.5	6
66	Local lunar gravity field analysis over the South Poleâ€Aitken basin from SELENE farside tracking data. Journal of Geophysical Research, 2012, 117, .	3.3	5
67	Two-stage development of the lunar farside highlands crustal formation. Planetary and Space Science, 2016, 120, 43-47.	1.7	5
68	Rotational effect as the possible cause of the east-west asymmetric crater rims on Ryugu observed by LIDAR data. Icarus, 2021, 354, 114073.	2.5	5
69	Modeling of 3D trajectory of Hayabusa2 re-entry based on acoustic observations. Publication of the Astronomical Society of Japan, 2022, 74, 308-317.	2.5	5
70	Seismic Tremors and Their Relation to Cryosphere Dynamics in April 2015 around the Lützow-Holm Bay, East Antarctica. International Journal of Geosciences, 2017, 08, 1025-1047.	0.6	4
71	Site selection for the Hayabusa2 artificial cratering and subsurface material sampling on Ryugu. Planetary and Space Science, 2022, 219, 105519.	1.7	4
72	Effect of Phase Pattern of Antennas Onboard Flying Spin Satellites on Doppler Measurements. IEEE Transactions on Aerospace and Electronic Systems, 2011, 47, 405-419.	4.7	3

#	Article	IF	CITATIONS
73	Characteristic atmosphere–ocean–solid earth interactions in the Antarctic coastal and marine environment inferred from seismic and infrasound recording at Syowa Station, East Antarctica. Geological Society Special Publication, 2013, 381, 469-480.	1.3	3
74	Characteristics of non-tectonic tremors around the Lützow-Holm Bay, East Antarctica, during 2013–2015. Polar Science, 2019, 19, 77-85.	1.2	3
75	Alignment determination of the Hayabusa2 laser altimeter (LIDAR). Earth, Planets and Space, 2021, 73, .	2.5	3
76	Modeling an international co-operative global complementary production system. Computers and Industrial Engineering, 1994, 27, 205-208.	6.3	2
77	Quantitative measurement method for impact basin characteristics based on localized spherical harmonics. Icarus, 2014, 228, 315-323.	2.5	2
78	Lunar mare volcanism: lateral heterogeneities in volcanic activity and relationship with crustal structure. Geological Society Special Publication, 2015, 401, 127-138.	1.3	2
79	Global Distribution and Geological Context of Coâ€Existing Occurrences of Olivineâ€Rich and Plagioclaseâ€Rich Materials on the Lunar Surface. Journal of Geophysical Research E: Planets, 2022, 127, .	3.6	2
80	Same-beam VLBI observation of SELENE. , 2009, , .		1
81	Usability of lunar reflectance model based on SELENE/SP for planned HISUI radiometric calibration. , 2013, , .		1
82	Four-way Doppler tracking for lunar gravity measurements executed by Kaguya and its relay satellite: Okina. , 2009, , .		0
83	Overview of Differential VLBI Observations of Lunar Orbiters in SELENE (Kaguya) for Precise Orbit Determination and Lunar Gravity Field Study. , 2010, , 123-144.		0
84	Albedo Observation by Hayabusa2 LIDAR: Instrument Performance and Error Evaluation. , 2016, , 49-64.		0